HOSTED BY

ELSEVIER

Available online at www.sciencedirect.com

ScienceDirect

Journal of Magnesium and Alloys 4 (2016) 89–98
www.elsevier.com/journals/journal-of-magnesium-and-alloys/2213-9567

Full Length Article

Texture evaluation in warm deformation of an extruded Mg–6Al–3Zn alloy

M. Kavyani [a], G.R. Ebrahimi [a], M. Sanjari [b], M. Haghshenas [c,*]

[a] Department of Materials and Polymer Engineering, Hakim Sabzevari University, Sabzevar, Iran
[b] Department of Mining and Materials Engineering, McGill University, Montreal, Canada
[c] Department of Mechanical Engineering, University of North Dakota, Grand Forks, USA

Received 10 May 2016; accepted 17 May 2016

Available online 27 May 2016

Abstract

To assess the effect of strain and strain rate on texture evolution of an extruded Mg–6Al–3Zn alloy, compression tests were carried out. Samples were prepared in the extrusion direction (ED) and normal direction (ND). The compression tests were performed at 250 °C and with different strain rates of 0.01 sec^{-1} and 1 sec^{-1} and different strains. Microstructural observation and texture investigation show that at early stages of deformation, extension twins lead to the development of strong basal texture intensity along rolling direction (RD) in ED samples and contraction twins result in texture evolution along transverse direction (TD) in ND samples. Also, microstructural investigation at high strains reveals that dynamic recrystallization occurs in both samples and consequently the basal texture intensity has been decreased.

Keywords: Extruded magnesium alloy; Deformation texture; Twinning; Recrystallization

1. Introduction

Poor formability of magnesium alloys is owing to the absence of independent slip systems at room temperature according to the von Mises criterion. Main slip systems in magnesium and its alloys are: basal slip $\langle a\rangle$; $\{0002\}\langle 11\bar{2}0\rangle$, prismatic slip $\langle a\rangle$; $\{10\bar{1}1\}\langle 11\bar{2}0\rangle$, second order pyramidal slip $\langle c+a\rangle$; $\{11\bar{2}2\}\langle 11\bar{2}3\rangle$. Beside these slip systems, mechanical twinning plays important roles in plastic deformation of magnesium alloys. The main twinning systems in magnesium alloys include $\{10\bar{1}2\}\langle 10\bar{1}1\rangle$ extension twins, $\{10\bar{1}1\}\langle 10\bar{1}2\rangle$ contraction twins and $\{10\bar{1}1\}-\{10\bar{1}2\}$ double twins [1,2].

Lee et al. [3] showed that plastic deformation of magnesium alloys can be slip-dominant or twinning-dominant depending on loading, texture and microstructure. The influence of twin on strain-hardening behavior of magnesium and its alloys has been investigated in the literature [4,5]. Depending on the loading directions, mechanical twinning cooperates with the dislocations glide to the total deformation [6]. The role of loading direction is signified with respect to the c-axis of the HCP unit cell in that, under stress states in which the crystal structure elongates along the c-axis, extension twinning is activated [7] which results in adopting the elongation along the c-axis by an 86° rotation of crystal structure about the $\langle 1\bar{1}20\rangle$ directions on the $\{10\bar{1}2\}$ planes [8]. The reported critical resolved shear stress (CRSS) value for this mechanism is in the range of 8–12 MPa [9]. Another mechanism accommodating strain along the c-axis is secondary pyramidal slip, $\langle c+a\rangle$ slip, which its CRSS is in the range of 40–100 MPa [10,11]. Therefore, by loading textured magnesium parallel to the basal plane during compression, which tends to elongation along the c-axis, plastic deformation generally begins with extension twinning. In these cases the Schmid factor for basal slip mechanisms is almost zero; therefore, twins are activated. However, the twin-induced deformation is limited to low strains as grains volume is saturated by the extension twinning, *i.e.*, the whole grain reorients by a rotation of 86° about the $\langle 1\bar{1}20\rangle$ [2]. For instance, in compressive loading along the rolling direction or extrusion direction of wrought magnesium products tensile twins could be activated leading to elongation along the c-axis [12]. On the other hand, there are another stress states leading to contraction of the HCP structures along the c-axis. Under these conditions, a very limited volume of crystal deforms by twinning in order to compensate the contraction along the c-axis which is known as contraction twinning [12]. Comparing to extension twinning, contraction twinning is largely ineffective during deformation

* Corresponding author. Department of Mechanical Engineering, University of North Dakota, Grand Forks, USA.
E-mail address: meysam.haghshenas@engr.und.edu (M. Haghshenas).

http://dx.doi.org/10.1016/j.jma.2016.05.002

due to its high CRSS value. An example of loading conditions resulting in contraction of crystal along the c-axis is the tension loading along the extrusion direction, ED, or the rolling direction, RD, in an extruded and rolled magnesium products, respectively. In both cases the c-axis is perpendicular to the RD and ED. Thus, because of the Poisson's effect, tension loading along these two directions is associated with contraction along the c-axis. As a result, extension twins and contraction twins can produce elongation or contraction along crystal c-axis.

It is worth mentioning that some parameters such as initial texture, grain size, strain, strain rate and temperature have a significant effect on twinning behavior. For example, if c-axis of grains is perpendicular to the compression direction, grains are reoriented by twinning during deformation so that their c-axis becomes parallel to the compression direction [13,14]. Deformation twins are formed more conveniently in larger grains due to the lack of grain boundaries [15]. Choi et al. [16] studied the influence of initial direction of compression test for a hot-rolled AZ31 alloy. They found that work hardening rate of specimens having a compression axis parallel to the ND is greater than the specimens with a compression axis parallel to the RD. Then, they reported a rapid rotation from the ND to RD for the specimen parallel to the RD in low strains such as 0.04 due to reorientation of the crystal lattice by twining. Prasad and Rao [17] investigated the influence of initial texture on the deformation behavior of AZ31 in compression test. The compression samples axis was prepared in three directions: parallel to the ND, RD and TD. Their studies show that the slip systems for the RD, TD and ND are first-order and second-order pyramidal slips, first order pyramidal slip and second order pyramidal slip, respectively. In other words, both first-order and second-order pyramidal slip systems are activated when the sample axis is parallel to the RD while first order pyramidal slip and second order pyramidal slip can simply get activated as the sample axis is parallel to the rolling direction and normal direction.

To improve the formability and ductility, the deformation of magnesium alloys is usually performed at elevated temperatures. Hence, it is very important to fully understand the deformation behavior of magnesium alloys under various deformation conditions. Therefore, some studies were performed to understand the flow stress behavior and microstructure evolution under hot deformation process [18–20]. Maksoud et al. [18] studied the effect of strain rate and temperature on microstructure evolution of magnesium alloys and showed that at elevated temperature and high strain rate the peak stress decrease while recrystallized grains size and their volume fraction increase. The influence of strain rate and temperature on flow stress and yield point depends on dominant deformation mechanism as well as loading path, texture and microstructure [21]. Klimanek and Pötzsch [19] studied the microstructure evolution during compression test and reported that microstructure evolution has a strong relationship with the initial state (grain size, texture and dislocation arrangement). The influence of initial texture and texture evolution during plastic deformation has been reported in the released literature [22,23]. Al-Samman [24] investigated the effect of temperature and strain on the texture and microstructure evolution of AZ31. They realized that with increasing strain at 200 °C, twins and shear bands are formed and by increasing the temperature to 400 °C random texture are developed along with prismatic texture $\{10\bar{1}0\}\langle 11\bar{2}0\rangle$. Although some studies have dealt with deformation behavior of magnesium and its alloys during uniaxial and plane strain compression, there is still insufficient knowledge and understating of dominant deformation mechanism during hot deformation. Besides, twinning and slip and dynamic recrystallization possess strong effects on both microstructure and texture during deformation of magnesium alloys at elevated temperatures. At high temperatures, recrystallization occurs in torsion, uniaxial compression, extrusion and equal channel angular pressing [25].

Since the deformation behavior of wrought magnesium alloys highly dependent upon initial texture and thermomechanical parameters, it is very important to evaluate and understand the mechanical behavior and microstructural evolution of magnesium alloys under compression loading in different loading directions. However, the mechanical behavior and deformation mechanisms of magnesium alloy AZ63 under hot compression have not yet been comprehensively investigated. Hence, this paper aims at studying the effect initial texture, strain and strain rate on the texture and microstructure evolution of an extruded Mg–6Al–3Zn during hot deformation.

2. Experimental procedure

Material used in this work was an extruded bar of Mg–6Al–3Zn alloy with diameter of 55 mm. To assess hot working behavior of the alloy, a Zwick/Roll tensile-compression test instrument equipped by an electric furnace with accuracy of ±5 °C was used. Cylindrical specimens with diameter of 8 mm and length of 12 mm were prepared in two directions for compression test: ED samples in which compression direction (CD) is parallel to extrusion direction and ND samples in which compression direction is perpendicular to extrusion direction (Fig. 1). Hot compression tests were carried out at 250 °C and strain rate of 0.01, 0.1, 1 s^{-1} and strains of 0.06, 0.75, 0.1, 0.2 and 0.6. Upon compression the samples were quenched in cold water for further microstructural investigations. The microstructures were studied by an Olympus GX51 optical microscope after being etched in a solution of picric acid (4.2 g), water (10 ml), acetic acid (10 ml) and ethanol (70 ml).

The macro-texture was evaluated by XRD technique using a Bruker D8 diffractometer with a Cu Ka source. The orientation distribution function (ODF) was constructed from the incomplete pole figures of, {00.2}, {10.0} and {10.1} using the

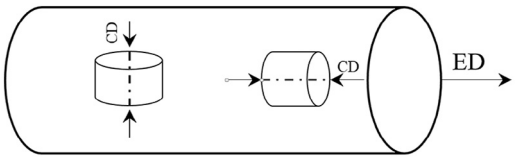

Fig. 1. Schematic illustration of compression samples prepared from extruded bar.

arbitrary defined cell (ADC) method by TexTools software. Recalculated pole figures as well as the distribution of basal planes were then derived from the ODFs.

3. Results and discussion

3.1. Flow behavior

As seen in true stress–true strain curves in Fig. 2, the flow stress of ED and ND samples increases to a peak value and then decreases gradually to finally attain a steady state typically. Decrease in the stress after maximum stress is a representative of work softening which can be ascribed to recrystallization phenomenon [26]. The steady state behavior in Fig. 2a is attributed to the equilibrium state between work hardening and DRX softening.

Fig. 2a and 2b show that yield stress in ED samples is less than ND samples at the same strain (dashed line in Fig. 2); this is attributed to the ease of activation of twinning in ED samples. After yield stress is reached, the slope of work hardening area increases linearly with increasing stress at the first stage of deformation, as observed in Fig. 2. The presence of yield point at lower stresses and linear behavior of work hardening both confirm the occurrence of the extension twins [1,2,16]. On the other hand, flow curve of ND samples is concave down revealing that the basal slip is dominant. There are two reasons for this behavior; the first is activity of pyramidal slip system, which can lead to proper orientation of crystal planes for basal slip as second slip mechanism [16,27,28]. The latter is related to the presence of contraction twins and double twins result in the activation of the basal slip systems. Barnett [2] and Kabirian et al. [12] reported that contraction and double twins contribute to the plastic deformation in ND samples.

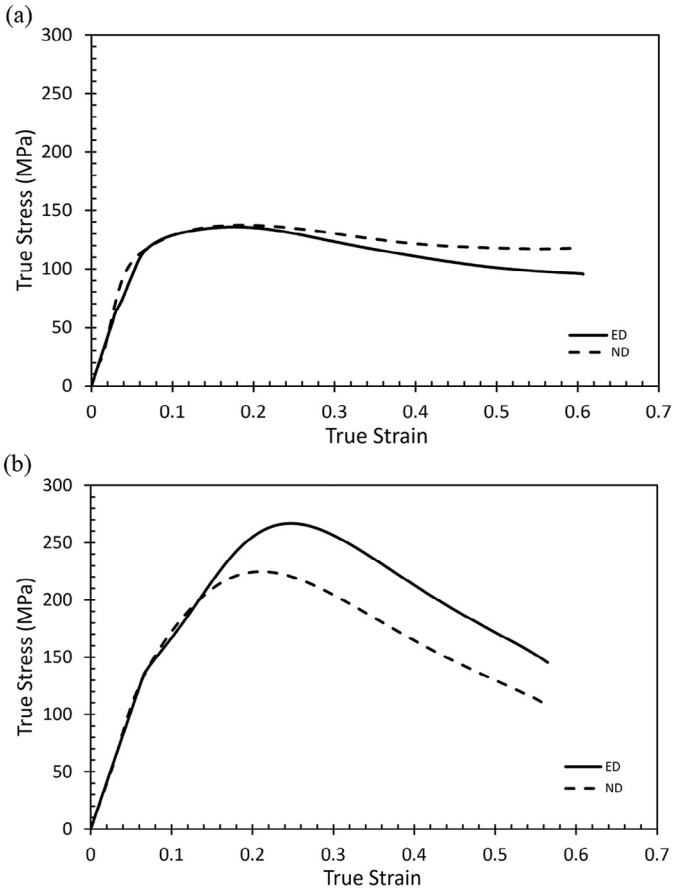

Fig. 2. True stress–true strain curves for ND and ED at 250 °C and strain rates: (a) 0.01 sec^{-1} and (b) 1 sec^{-1}.

Fig. 2a shows that the peak stress of ND samples is slightly higher than ED samples owing to the fact that the role of extension twins weakens as strain rate decreases. Also, shearing the grains by contraction and double twins in ND samples increases the maximum stress because of the Hall–Petch effect [29]. Therefore, the peak stress of ND samples and the equilibrium region of stress are slightly higher than ED samples. Similar behavior was reported by Zhang [30] and Knezevic et al. [28]; they assessed the effect of deformation twinning on the texture evolution and strain hardening of AZ31 magnesium alloy. Higher strain rate leads to greater strain hardening in ED samples, comparing to ND samples; thus, maximum stress of ED samples is higher than ND samples (see Fig. 2b). This can be contributed to easier formation of extension twins at high strain rate in ED and also lattice rotation by twinning lead to slip restriction and increasing work hardening. Hence, owing to the increase in work hardening, the peak stress increases and recrystallization delays. As a result of increasing dislocation density due to dislocation pile-up in the twinning boundary, more sessile dislocations are formed (Basinski effect). Barnett [2], Jiang et al. [4] and Dixit et al. [31] suggested the role of extension twin in increasing peak stress. In contrast, in ND samples due to contraction and double twins and favorite orientation of crystal planes, dislocations' easy slip becomes possible and therefore dynamic recrystallization starts at lower strains [21]. By comparing true stress–true strain curves in Fig. 2a and 2b, it can be concluded that the ductility increases with increase in strain rate. This behavior can be attributed to the higher probability of activation of $\langle c+a \rangle$ pyramidal slip systems at higher strain rates. Asgari et al. [32] reported such behavior in simulation analysis of texture formation and deformation mechanisms of rolled AZ31B magnesium alloy under dynamic loading.

3.2. Work hardening behavior

To study the work hardening behavior of ED and ND samples, the strain hardening diagram was drawn at 250 °C and strain rate of 1 sec^{-1}, as indicated in Fig. 3. Three distinct strain hardening stages of ED samples (as marked by dotted line in Fig. 3). At first, the work hardening rate decreases with increase in strain (stage 1), then increases to maximum peak (stage 2) and finally decreases again to corresponding strain of maximum point in the true stress–true strain ($\varepsilon \cong 0.25$ in Fig. 2b) (stage 3). Therefore, for ED samples, hardening firstly drops and then increases to a maximum before falling off again and a hump was formed on the diagrams, suggesting that twinning is the dominant deformation mechanisms in the samples [33,34]. As can be seen in the work hardening of ND samples, the strain hardening rate decreases continuously with increasing strain.

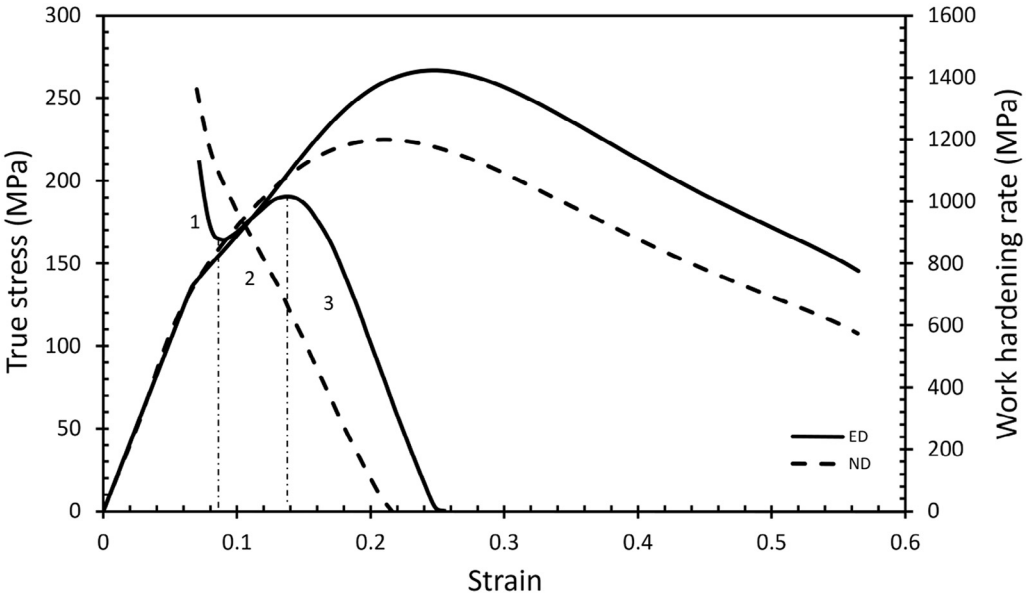

Fig. 3. Hardening diagram (strain hardening rate versus strain) for ED and ND samples at 250 °C and 1 sec^{-1}.

At low temperatures the basal slip is dominant owing to the lack of active slip systems (non-basal slips). Also extension twins play a significant role in deformation and accommodating plastic strain along HCP lattice c axis; in the present study due to dominant basal texture (0002) in ED samples, compression loading perpendicular to c-axis leads to activation of extension twins $\{10\bar{1}2\}$. For ED samples, at the initial region of hardening curve, where the strain-hardening rate decreases, deformation is mainly accommodated by slip and formation of $\{10\bar{1}2\}$ extension twins. Development of extension twins lead to lattice rotation by 86° and the number of extension twins increase to the maximum amount [35]; this is in agreement with results reported by Jiang et al. [4] and Barnett [1]. The increase in the strain-hardening rate, in the next step, can be ascribed to the interaction between twinning systems and twins–dislocations as well. Upon formation of extension twins, the twin boundaries hinder dislocations' motion and this results in dislocations' pile-up. The other factor that may contribute to the hardening behavior is the formation of twin intersections owing to the interaction between twins. In fact, interaction between twinning systems would contribute to the hardening. Both dislocation pile-up and twin intersection can increase the strain-hardening rate [33,34,36]. In the next step of hardening due to crystal lattice orientation the contraction twins $\{10\bar{1}1\}$ and double twins $\{10\bar{1}1\}-\{10\bar{1}2\}$ are formed. Contraction twins and double twins lead to lattice rotation by 56° and 38° respectively, which provide favorite orientation for basal slip systems. Knezevic et al. [28] showed that CRSS for activation of contraction twins is more than that of extension twins. Therefore, any increase in the work hardening up to this step provides enough stress concentration for activating contraction twins. Due to saturation and coalescence of twins, which happens at the peak of the strain rate hardening curves, the interaction between twinning systems decrease and therefore they cannot possibly act as barriers to dislocations motion. This may result in decreasing the strain-hardening rate as reported by some researchers [33,34]. Since deformation was performed at high temperature, cross slip and activation of non-basal slip systems could have occurred and therefore the hardening rate decreases after the peak point. Sarker and Chen [36] investigated the work hardening of AM30 magnesium alloy and showed that volume fractions of contraction twins are less than extension twins. Thus, decreasing twins density decrease their role as barrier to the dislocation motion and subsequently the work hardening rate decreases significantly in the third step. The hump formation in the hardening diagrams and its broadening with increase in strain rate is related to the change of deformation mechanisms and possible activation of non-basal slip systems such as pyramidal $\langle c+a\rangle$ system [34]. Jiang et al. [4] and Asgari et al. [33,37] reported three steps of hardening for loading along extrusion direction of magnesium alloys.

As seen in Fig. 3, in the case of ND samples the work hardening rate is dropping thoroughly. This can be attributed to compressive loading which is perpendicular to the basal planes, therefore contraction and double twins are formed. As mentioned before, these twins are more favorite places for the formation of basal slip; therefore, increase in the strain leads to decrease in work hardening rate significantly. Consequently, hardening diagram of ND samples is the same as the third step of ED samples hardening diagram. Knezevic et al. [28] observed such behavior in hardening diagrams of hot compression test on the rolling direction and normal direction samples.

3.3. Microstructure analysis

Microstructural observations clearly show the occurrence and development of various twins as were predicted by strain-hardening diagram. As shown in Fig. 4a, extension twins with thick and lenticular morphology are increasing with increase in strain in ED samples. At the strain of 0.1, in which maximum shear strain is induced by twinning along c-axis, a maximum

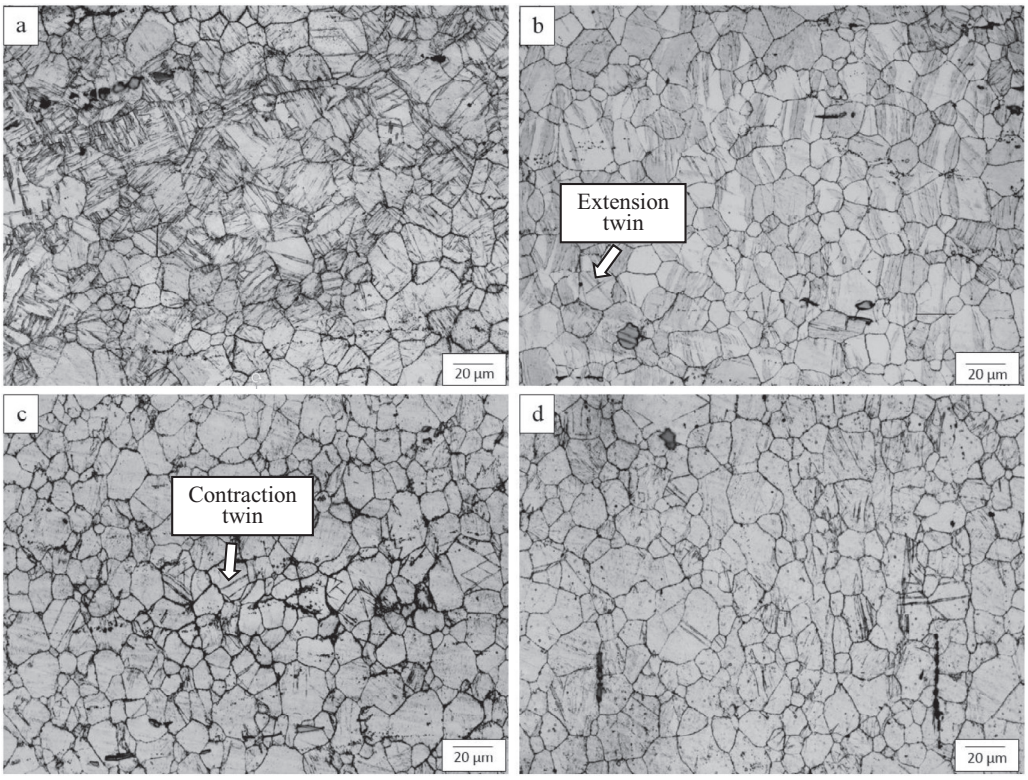

Fig. 4. Optical microstructures of the ED sample upon compression at 250 °C and strain rate of 1 sec^{-1} at true strains of (a) 0.075, (b) 0.15, (c) 0.25, and (d) ND sample at true strain of 0.1.

volume fraction of extension twin is achieved. However, in Fig. 4b, the amount of extension twin decreased as strain increased and only contraction twins with thin and extended morphology are observed at the higher strains. Extension and contraction twins were reported by Koike et al. [38] during tensile testing on the AZ31 magnesium alloy and other researches [2,23,39]. Microstructural observations in ND samples represent the presence of contraction twins at the early stages of deformation (see Fig. 4d).

As seen in Fig. 2, upon reaching peak stress dynamic recrystallization takes place, however, it is postponed with increasing strain rate (Fig. 2b). Here, driving force for both recrystallization and work hardening increases; however, the latter is the dominant one. In other words, work hardening caused by piled-up dislocations overcomes work softening due to dislocation-free grains nucleation. Therefore, both strain and peak stress does increase with increasing strain rate. The reason for increasing peak stress in large stresses is related to pyramidal slip. The effect of strain on the recrystallization was reported by Fan [40] and Al-Samman [41].

Microstructural observations at 250 °C and strain rates of 0.01 sec^{-1} and 1 sec^{-1} show that work hardening is bigger in ED samples than in ND samples while volume fraction and amount of recrystallized grain in ED samples is lower than ND samples. As shown in Fig. 5, at strain rate of 0.01 sec^{-1} (Fig. 5a and b) the grain size and the number of recrystallized grains are similar to each other while in the strain rate of 1 sec^{-1} (Fig. 5c and d) the ED samples grain size is smaller than ND samples. According to the true stress–true strain curve in Fig. 2a at the strain rate of 0.01 sec^{-1}, the flow stress of both samples is similar to each other. However, by increasing the strain rate to 1 sec^{-1}, the peak stress of ND samples is appeared at lower strains compared to ED samples. Consequently, recrystallization occurs earlier in ND samples resulting in larger volume fraction of recrystallized grains than ED samples. Microstructures comparison at different strain rates shows that high strain rate provides finer grain size with respect to low strain rate. In other words, the grain size at the strain rate of 1 sec^{-1} is finer than of 0.01 sec^{-1}. Furthermore, increasing dislocation density and twin formation results in storing a larger amount of energy in grain boundaries and twin boundaries. Therefore, more favorite locations are provided for recrystallization nucleation. However, in high strain rates, driving force for grain growth is declined, thus the grain size is reduced. According to Wang et al. [42], twins possess a significant role on DRX nucleation during hot deformation in magnesium alloy. DRX nucleation can occur on twin boundary and within twining since there is a great deal of stored energy than the matrix as these are preferred locations for DRX nucleation.

3.4. Texture analysis

3.4.1. Initial texture

Fig. 6 shows the texture of the extruded Mg–6Al–3Zn magnesium alloy used in this study. As observed, the basal planes (0002) are perpendicular to the RD (Rolling direction = Extrusion Direction). The basal planes rotate 10–30° along transverse

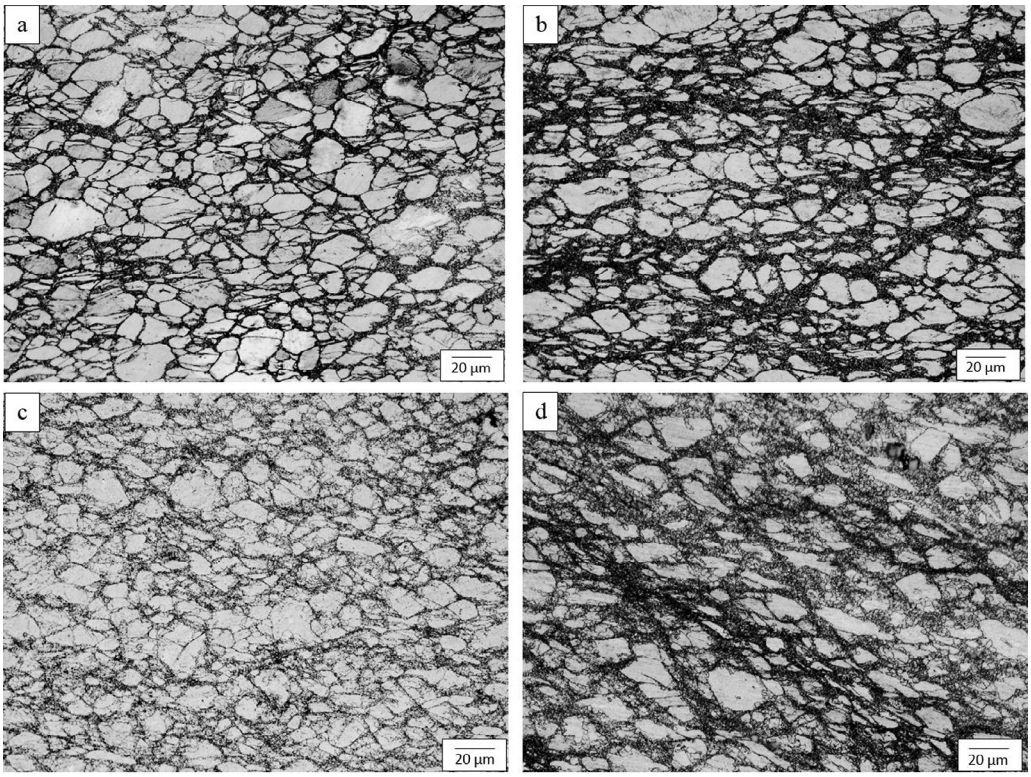

Fig. 5. Optical microstructures upon compression at 250 °C: (a) ED, strain rate of 0.01 sec^{-1}; (b) ND, strain rate of 0.01 sec^{-1}; (c) ED, strain rate of 1 sec^{-1}; and (d) ND, strain rate of 1 sec^{-1}.

direction so that c-axis of grains are perpendicular to the extruded direction. In rolled (or extruded) materials, shear-bands occur at ~35° to the rolling (extruded) plane and parallel to the transverse direction. Formation of shear bands may change the deformation texture by rotating the material along the transverse direction and this may change texture intensity [43]. Wang et al. [42] reported that when basal poles are nearly parallel to the ND, non-basal dislocation $\langle a \rangle$ slip accommodate the strain along TD. However, this texture is a common texture in the extruded magnesium alloy [14].

3.4.2. *The effect of strain on the texture of ED sample*

Fig. 7 reveals pole figures upon compression of ED samples at 250 °C and strain rate of 1 sec^{-1}. As seen, the basal poles of the grains are in the center of pole figure. It indicates that the basal texture (0002) is dominant in which the grains c-axis are nearly perpendicular to the RD; that is, the basal planes align with the compression axis. The subsequent loading reorient the basal plane toward RD (Fig. 7b) leading to decrease in the basal texture intensity.

According to Fig. 7a, in ED samples the basal planes are parallel to the compression axis at first. High intensity of basal texture is due to extension twin and basal slip, since there were basal slip and extension twins $\{10\bar{1}2\}$ at the beginning of the deformation; also extension twins seem to play a dominant role on the texture evolution at the early stages of the compression of the ED samples. Choi et al. [16] observed extension twins activity and basal slip in the early stages of deformation during

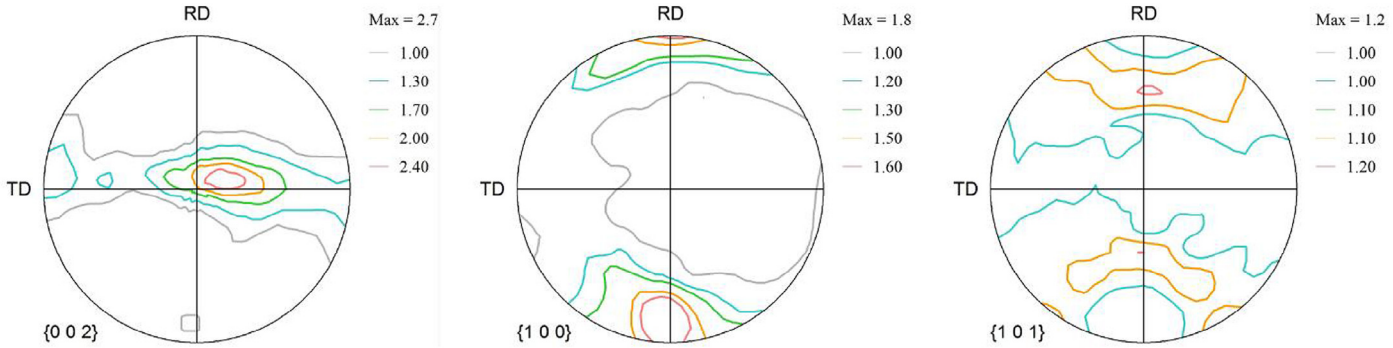

Fig. 6. Pole figures of the extruded Mg–6Al–3Zn used in this study.

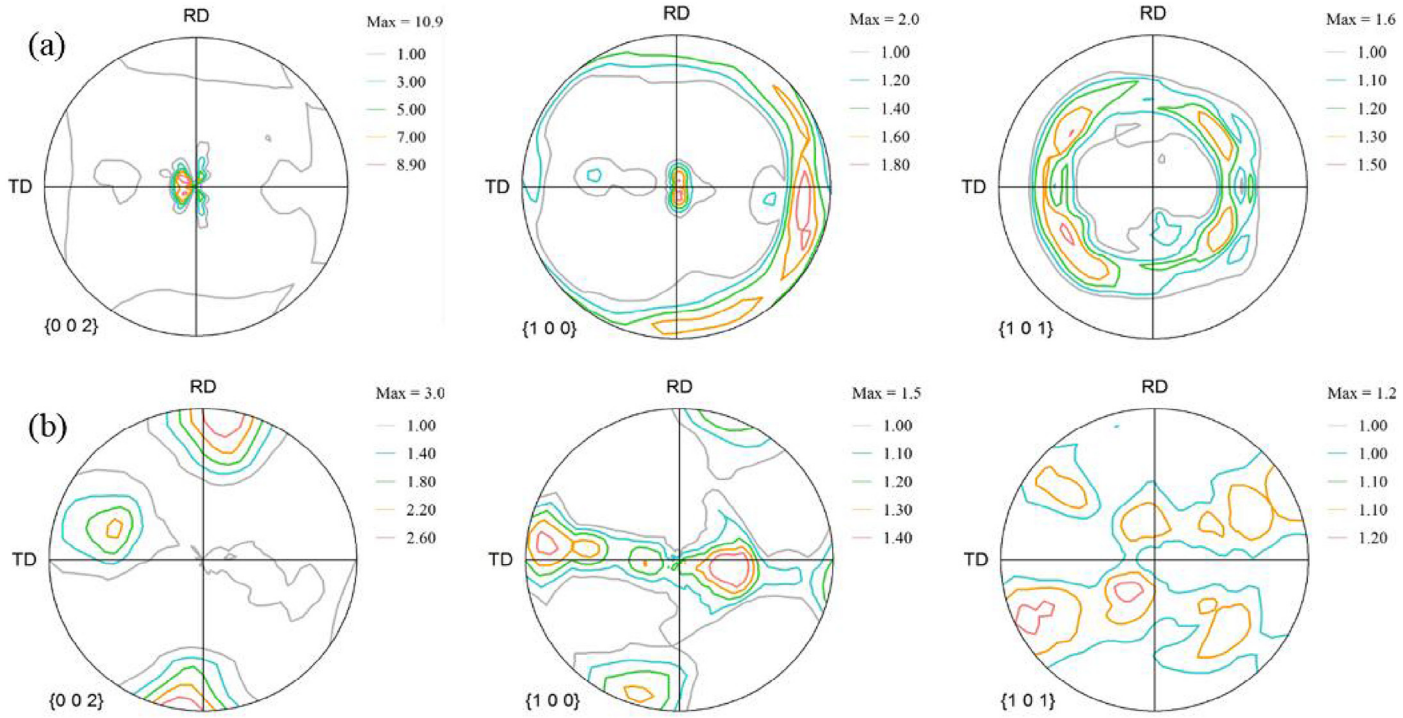

Fig. 7. Pole figures of ED samples upon compression at 250 °C and strain rate of 1 sec^{-1}: (a) strains: 0.06, and (b) strains: 0.1.

uniaxial compression. Kabirian et al. [12] described that only basal slip $\langle a \rangle$ with low CRSS and extension twin formed at the beginning of the deformation in the ED samples; however, the other mechanisms have no considerable effect on texture evolution. As indicated in Fig. 7b, with increasing strain, more twins are activated which accommodate plastic strain along c-axis. Since loading direction is perpendicular to the c-axis (or parallel to the basal planes), the type of twins are extension twins $\{10\bar{1}2\}\langle 11\bar{2}0\rangle$. Activation and development of extension twin [39] lead to reorientation of crystal lattice by 86° about

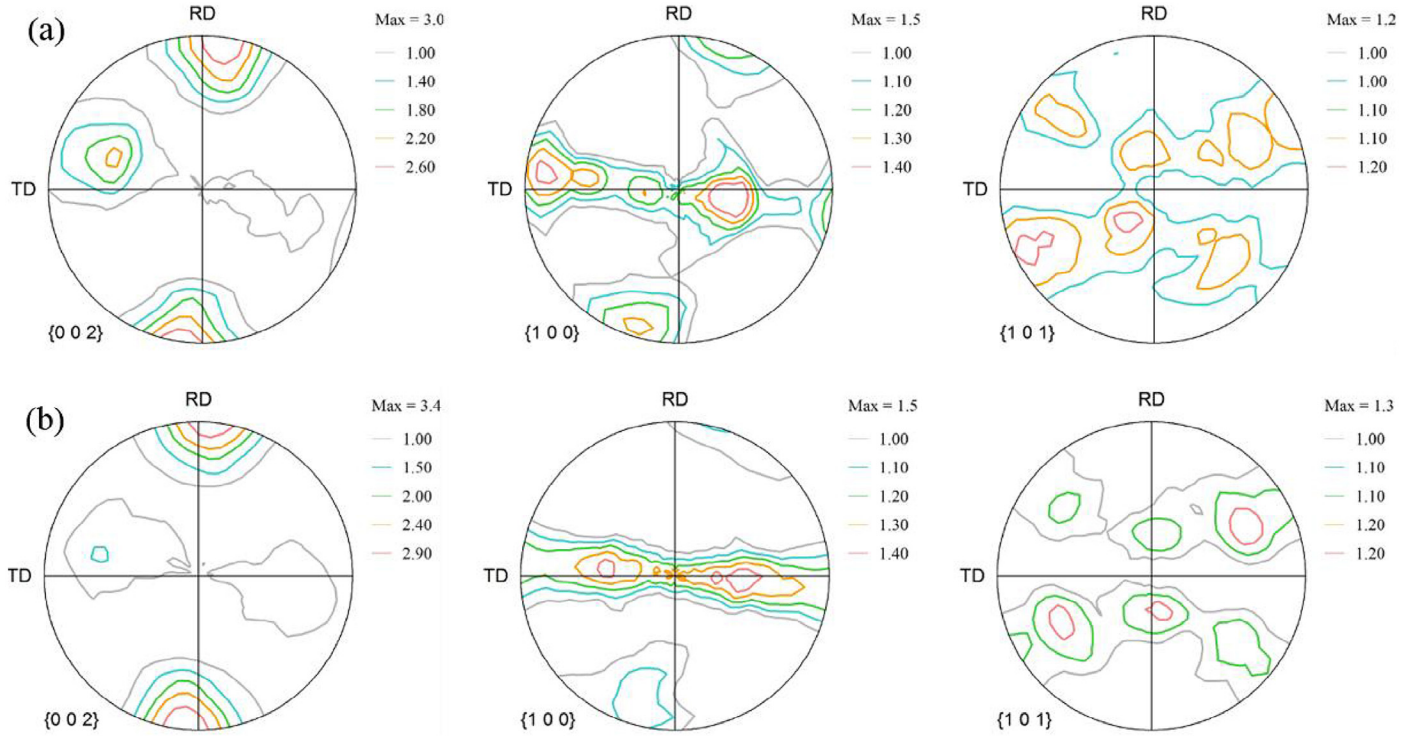

Fig. 8. Pole figures of ED samples upon compression at 250 °C and strain of 0.1: (a) strain rate: 0.1 sec^{-1}, and (b) strain rate: 1 sec^{-1}.

$\langle 11\bar{2}0 \rangle$ which inclines the basal poles toward rolling direction or perpendicular to the loading direction. In other words, compressive loading reorients the grain c-axis parallel to the compression direction. Furthermore, in the initial steps of deformation, extension twin is activated due to lower CRSS than contraction and double twin. Some studies [39,44,45] observed the presence of extension twins at the beginning of ED compression.

3.4.3. *The effect of strain rate on the ED samples*

Fig. 8 shows the effect of strain rate on the texture evolution during hot compression of ED samples at 250 °C and the

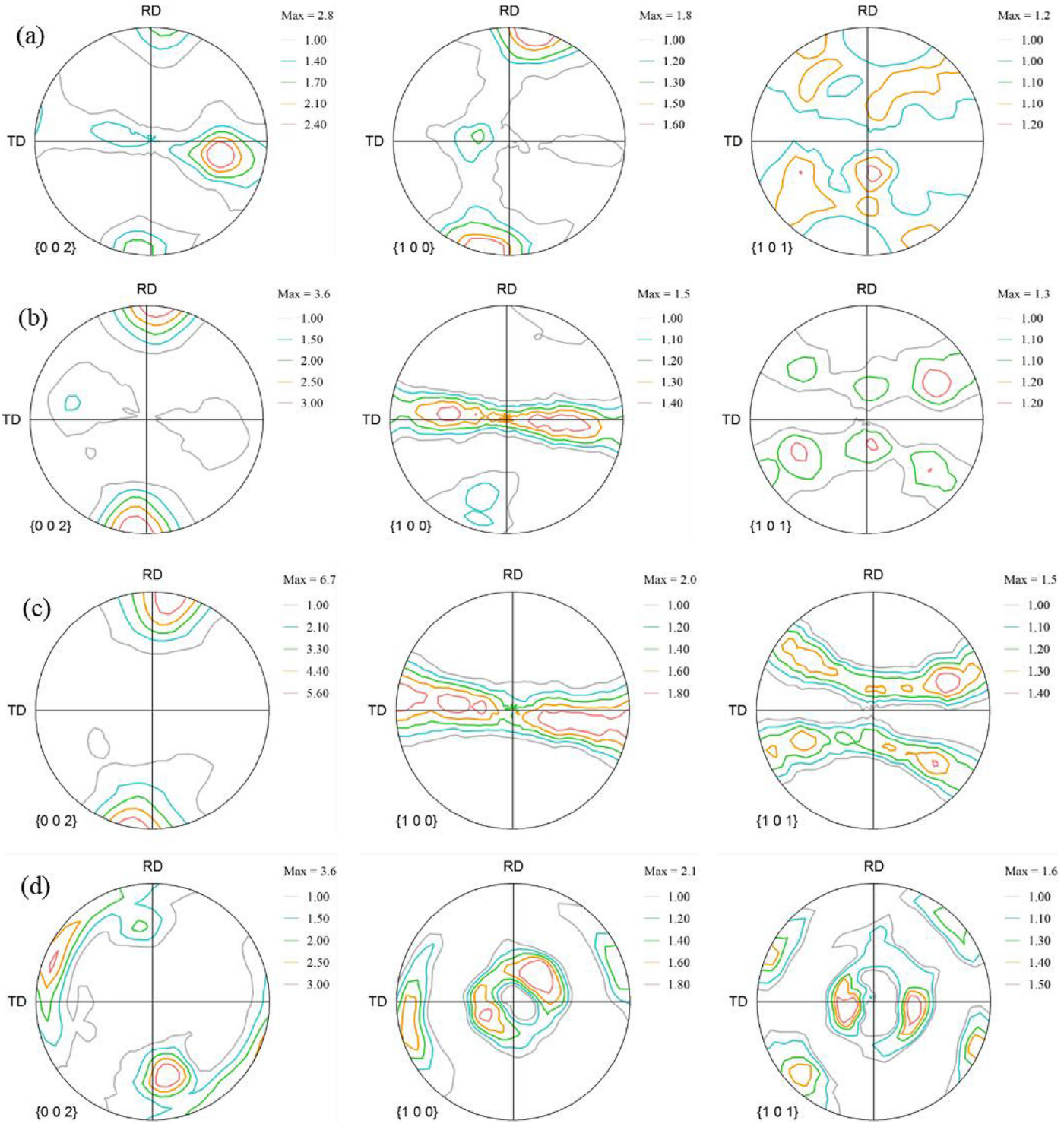

Fig. 9. Pole figures of ND samples upon compression at 250 °C and strain rate of 1 sec^{-1}: (a) strain: 0.075, (b) strain: 0.1, (c) strain: 0.2, and (d) strain: 0.6.

strain of 0.1. It can be found that raising the strain rate increases in texture intensity by increasing the amount of twin activity. Thus, as indicated in Fig. 8a and b, the basal poles intensity is increased along RD with increase in strain rate leading to strong basal texture, therefore, pole density of the basal planes align with compression direction. Styczynski et al. [22] reported that increasing the strain rate results in the strong basal texture.

3.4.4. *The effect of strain on the ND samples*

The pole figure of ND samples upon hot compression at 250 °C and strain rate of 1 s^{-1} are shown in Fig. 9. At the early stages, basal planes are oriented toward TD (Fig. 9a) and then by increasing the strain, basal poles align with RD (Fig. 9b and c) and after that basal poles are reoriented again toward the center of the figure (Fig. 9d).

Since the compression direction is perpendicular to the basal plane (parallel to the c-axis), there is a possibility to activate the contraction twins $\{10\bar{1}1\}\langle 11\bar{2}0\rangle$ and double twin $\{10\bar{1}1\}-\{10\bar{1}2\}$ which can result in reorientation of crystal lattice by 56° about $\langle 11\bar{2}0\rangle$ and 38° about $\langle 11\bar{2}0\rangle$, respectively [4,39]. Therefore, twins provide favorite orientation for basal slip. As observed in Fig. 9a, basal planes are orienting along TD. Basal planes may orient by 56° along TD in comparison with the initial texture (Fig. 6), which reveals the contraction twin activity [46]. As seen in Fig. 9a and b, increasing the strain results in more twin activity and thus texture changes remarkably. As a result, poles align with RD and texture intensity becomes stronger by increasing strain. Change in texture can be associated with two reasons: the first is that as the strain increases, many grains are reoriented so that extension twins can be activated resulting in reorientation of basal planes by 86° along RD. It was suggested by Meng et al. [46] that at the beginning of the deformation, the activity of contraction twins leads to changes in as-extruded texture; therefore, applied strain causes reorientation of the basal planes by extension twins. The second reason can be attributed to activation of pyramidal $\langle c+a\rangle$ slip. Based on investigations performed by Kabirian and Agnew [12,13], pyramidal $\langle c+a\rangle$ slip will allow c-axis compression and, hence, the basal poles may rotate away from the compression axis (*i.e.* toward the "rolling direction" in plane strain compression). Fig. 9d indicates that one pole inclined toward the center of the figure and the other pole reoriented to the transverse direction. As observed in the true stress–true strain in Fig. 2b, recrystallization occurred at the strain of 0.6. There is a possibility of the activation of the prismatic slip at high strains and elevated temperatures. As seen in the pole figure $\{100\}$ there is no change in the texture intensity of the prismatic plane as the strain increased to 0.6. Therefore, it can be concluded that at the strain of 0.6 the crystal orientation is favorite for prismatic plane activity. Recrystallization may result in the weakening of basal texture. Furthermore, sometimes resultant texture may be similar to the initial texture (as-extruded texture) but this texture possesses less intensity than initial texture. Similar observation [45,47–49] approved the effect of recrystallization on the weakening of the texture.

4. Conclusion

Warm deformation response of an extruded Mg–6Al–3Zn alloy was studied in this paper through compression testing. Here are the main findings:

- Increasing the strain in ED samples leads to an increase in the texture intensity of the basal planes (0002) perpendicular to the compression direction by formation and development of extension twins. In other words, the formation of the extension twins causes reorientation of grains with c-axis parallel to the compression direction and thus basal poles align with RD.
- As the strain rate in the ED samples increases, density of extension twins increases, and therefore the basal texture intensity of the basal plane (0002) along RD is enhanced.
- Increase in the strain in ND samples caused the formation and development of the contraction twins and double twins. Furthermore, increase in the pole density of the (0002) basal plane can be attributed to the pyramidal slip and extension twins' activity.

References

[1] M. Barnett, Mater. Sci. Eng. A 464 (2007) 1–7.
[2] M. Barnett, Mater. Sci. Eng. A 464 (2007) 8–16.
[3] M.-G. Lee, R. Wagoner, J. Lee, K. Chung, H. Kim, Int. J. Plasticity 24 (2008) 545–582.
[4] L. Jiang, J.J. Jonas, A.A. Luo, A.K. Sachdev, S. Godet, Scripta Mater. 54 (2006) 771–775.
[5] Y. Wang, J. Huang, Acta Mater. 55 (2007) 897–905.
[6] G. Proust, C.N. Tomé, A. Jain, S.R. Agnew, Int. J. Plasticity 25 (2009) 861–880.
[7] P. Partridge, Metall. Rev. 12 (1967) 169–194.
[8] B.C. Wonsiewicz, Plasticity of Magnesium Crystals, Massachusetts Institute of Technology, 1966.
[9] A. Chapuis, J.H. Driver, Acta Mater. 59 (2011) 1986–1994.
[10] R. Sanchez-Martin, M. Perez-Prado, J. Segurado, J. Bohlen, I. Gutierrez-Urrutia, J. Llorca, et al., Acta Mater. 71 (2014) 283–292.
[11] C.M. Byer, B. Li, B. Cao, K. Ramesh, Scripta Mater. 62 (2010) 536–539.
[12] F. Kabirian, A.S. Khan, T. Gnäupel-Herlod, Int. J. Plasticity 68 (2015) 1–20.
[13] S.R. Agnew, M.H. Yoo, C.N. Tomé, Acta Mater. 49 (2001) 4277–4289.
[14] S. Godet, L. Jiang, A. Luo, J. Jonas, Scripta Mater. 55 (2006) 1055–1058.
[15] M. Barnett, Z. Keshavarz, A. Beer, D. Atwell, Acta Mater. 52 (2004) 5093–5103.
[16] S. Choi, E. Shin, B. Seong, Acta Mater. 55 (2007) 4181–4192.
[17] Y. Prasad, K. Rao, Mater. Sci. Eng. A 432 (2006) 170–177.
[18] I.A. Maksoud, H. Ahmed, J. Rödel, Mater. Sci. Eng. A 504 (2009) 40–48.
[19] P. Klimanek, A. Pötzsch, Mater. Sci. Eng. A 324 (2002) 145–150.
[20] J. Tan, M. Tan, Mater. Sci. Eng. A 339 (2003) 124–132.
[21] S. Xu, W. Tyson, R. Eagleson, R. Zavadil, Z. Liu, P.-L. Mao, et al., J. Magnes. Alloys 1 (2013) 275–282.
[22] A. Styczynski, C. Hartig, J. Bohlen, D. Letzig, Scripta Mater. 50 (2004) 943–947.
[23] M. Barnett, M. Nave, C. Bettles, Mater. Sci. Eng. A 386 (2004) 205–211.
[24] T. Al-Samman, Acta Mater. 57 (2009) 2229–2242.
[25] L. Jin, D. Lin, D. Mao, X. Zeng, B. Chen, W. Ding, Mater. Sci. Eng. A 423 (2006) 247–252.
[26] R.-L. Xin, B.-S. Wang, Z. Zheng, G.-J. Huang, L. Qing, Trans. Nonferr. Metal. Soc. 20 (2010) 594–598.
[27] S. Xu, W. Tyson, R. Bouchard, R. Eagleson, Tensile and compressive properties for crashworthiness assessment of a large AZ31 extrusion. In Materials Science ForumTrans Tech Publ 527–532, 2009.

[28] M. Knezevic, A. Levinson, R. Harris, R.K. Mishra, R.D. Doherty, S.R. Kalidindi, Acta Mater. 58 (2010) 6230–6242.
[29] S.-G. Hong, S.H. Park, C.S. Lee, Acta Mater. 58 (2010) 5873–5885.
[30] D. Zhang, S. Li, Mater. Sci. Eng. A 528 (2011) 4982–4987.
[31] N. Dixit, K.Y. Xie, K.J. Hemker, K. Ramesh, Acta Mater. 87 (2015) 56–67.
[32] H. Asgari, J.A. Szpunar, A.G. Odeshi, Mater. Des. 61 (2014) 26–34.
[33] R. Korla, A.H. Chokshi, Scripta Mater. 63 (2010) 913–916.
[34] A.S. Khan, A. Pandey, T. Gnäupel-Herold, R.K. Mishra, Int. J. Plasticity 27 (2011) 688–706.
[35] L. Jiang, J.J. Jonas, A.A. Luo, A.K. Sachdev, S. Godet, Mater. Sci. Eng. A 445–446 (2007) 302–309.
[36] D. Sarker, D. Chen, Scripta Mater. 67 (2012) 165–168.
[37] H. Asgari, J. Szpunar, A. Odeshi, L. Zeng, E. Olsson, Mater. Sci. Eng. A 618 (2014) 310–322.
[38] J. Koike, Y. Sato, D. Ando, Mater. Trans. 49 (2008) 2792–2800.
[39] M.D. Nave, M.R. Barnett, Scripta Mater. 51 (2004) 881–885.
[40] X. Fan, W. Tang, S. Zhang, D. Li, Y. Peng, Acta Metall. Sin. 23 (2010) 334–342.
[41] T. Al-Samman, X. Li, S.G. Chowdhury, Mater. Sci. Eng. A 527 (2010) 3450–3463.
[42] Y. Xin, M. Wang, Z. Zeng, G. Huang, Q. Liu, Scripta Mater. 64 (2011) 986–989.
[43] P. Wilson, Recent Developments in the Study of Recrystallization, 2013.
[44] A. Jain, S. Agnew, Mater. Sci. Eng. A 462 (2007) 29–36.
[45] S. Abdessameud, D. Bradai, Can. Metall. Quart. 48 (2009) 433–442.
[46] L. Meng, P. Yang, Q. Xie, W. Mao, Mater. Trans. 49 (2008) 710–714.
[47] R. Cottam, J. Robson, G. Lorimer, B. Davis, Mater. Sci. Eng. A 485 (2008) 375–382.
[48] S. Ion, F. Humphreys, S. White, Acta Metall. Sin. 30 (1982) 1909–1919.
[49] F. Xiong, C. Davies, Strain path and temperature effects on texture and microstructure evolution of AZ31. In 2005 TMS Annual Meeting to TMS: 217–222, 2005.